

Surface effects on the energetic and spintronic properties of InP nanowires diluted with Mn: First-principles calculations

T. M. Schmidt

Instituto de Física, Universidade Federal de Uberlândia, Caixa Postal 593, Uberlândia, CEP 38400-902 Minas Gerais, Brazil

(Received 21 September 2007; revised manuscript received 13 November 2007; published 27 February 2008)

First-principles calculations have been used to investigate the impurity stability and the magnetic properties of Mn doped InP nanowires. The results reveal that the surface of the nanocrystals play a fundamental role on the impurity stability and on the magnetic properties of InP nanowires diluted with Mn. The formation energy of pairs of Mn impurities in unpassivated nanowires are lower than that of the bulk InP. Most of the Mn pair configurations present FM coupling and they prefer to be inside the nanowire and not on the surface. The origin of the ferromagnetic interaction in the nanowire is different from that of the bulk, and the ferromagnetic coupling is energetically more stable than the ferromagnetism in Mn doped bulk InP, making this nanostructure promising for spintronic applications.

DOI: [10.1103/PhysRevB.77.085325](https://doi.org/10.1103/PhysRevB.77.085325)

PACS number(s): 73.22.-f, 73.61.Ey, 75.30.Hx, 75.50.Pp

I. INTRODUCTION

Diluted magnetic semiconductors with nanocrystals have brought exciting technological and scientific developments. In particular, the discovery of ferromagnetism in III-V semiconductors doped with transition metal atoms has attracted considerable attention¹⁻⁸ due to their unique magnetic and magneto-optical properties. Due to the large surface-to-volume ratio of these nanostructures, of particular interest is the understanding of the unknown and hard to determine experimentally surface structure and their effects on the electronic and magnetic properties. InP nanostructured materials have also a great potential for fabrication of sensors, light emitting diodes, and field effect transistors.^{9,10} These materials are quasi-one-dimensional with electrons confined in two directions with small cross-section area. The new electronic, magnetic, and optical properties of these nanocrystals are mainly due to quantum confinement effects.

Mn doped bulk III-V semiconductor is known to be incorporated preferentially substitutional in the cation site. In InP, the d orbitals of the Mn dopant are positioned deep inside the valence band (VB), leaving the levels around the top of the VB with strong host p character and a small Mn d component. The magnetic coupling is due to p - d exchange. The understanding of the magnetic order on these III-V semiconductors is still in discussion.¹¹⁻¹⁵

In nanocrystals, the incorporation of impurities is a difficult task. The doping control is suggested to be in the adsorption of impurities during the growth.¹⁷ Calculations predict that impurities prefer to migrate toward the surface, including transition metal atoms as the Mn.¹⁶ This “self-purification” mechanism is mainly due to the proximity of the impurity to the surface. The Mn-related impurity states in nanocrystals are deeper as compared to that of bulk due to confinement effects. Consequently, the magnetic order in nanocrystals usually cannot be ascribed to a Zener-like model mediated by free holes as in bulk GaAs:Mn,¹⁸ neither by the RKKY picture.

In this work, our first-principles calculations show that in Mn doped unpassivated InP nanowires, different from what have been observed in some II-VI, IV-IV, and in passivated

III-V nanocrystals, the formation energy is lower than that of the bulk InP. The energetically more stable positions for the Mn atoms are inside the nanowire and not on the surface. Our results show that there is a Mn-induced impurity band inside the nanowire band gap, and the stabilization of the ferromagnetic interaction must be via a double exchange mechanism. Most of the Mn pair configurations studied here present ferromagnetic coupling, even with the Mn atoms near to the surface of the unpassivated nanowire, and they are energetically more stable than the ferromagnetism in bulk InP.

II. METHODOLOGY

Our total energy calculations are based on the density functional theory within the generalized gradient approximation for the exchange-correlation potential, with the electron-ion interactions described by ultrasoft pseudopotentials.¹⁹ A plane wave expansion up to a 385 eV cutoff energy (tests up to 500 eV have been performed), as implemented in the VASP code,²⁰ has been used. The nanowires have been constructed along the [111] direction using the supercell approach, in which the periodicity length is $\sqrt{3}a$, where a is the bulk lattice parameter. The wires present crystalline structure with six {110} planes forming a hexagonal cross section. All the geometries were optimized until the forces were less than 0.02 eV/Å. The relaxations have been handled by computing the Hellmann-Feynman forces using the conjugate gradient algorithm. The Pullay stress correction has also been taken into account. The Brillouin zone was sampled by $2k$ points along the nanowire axis. Tests on the sampling of the Brillouin zone have been performed up to five $5k$ points, showing a convergence after $2k$ points, even for the unpassivated nanowires. For the bulk InP, we use up to $10k$ points to sampling the Brillouin zone.²¹

III. RESULTS AND DISCUSSION

In order to understand the surface effects, we compare two types of nanowires. In one of them, we use a previous calculated nanowire,⁶ where all dangling bonds on the sur-

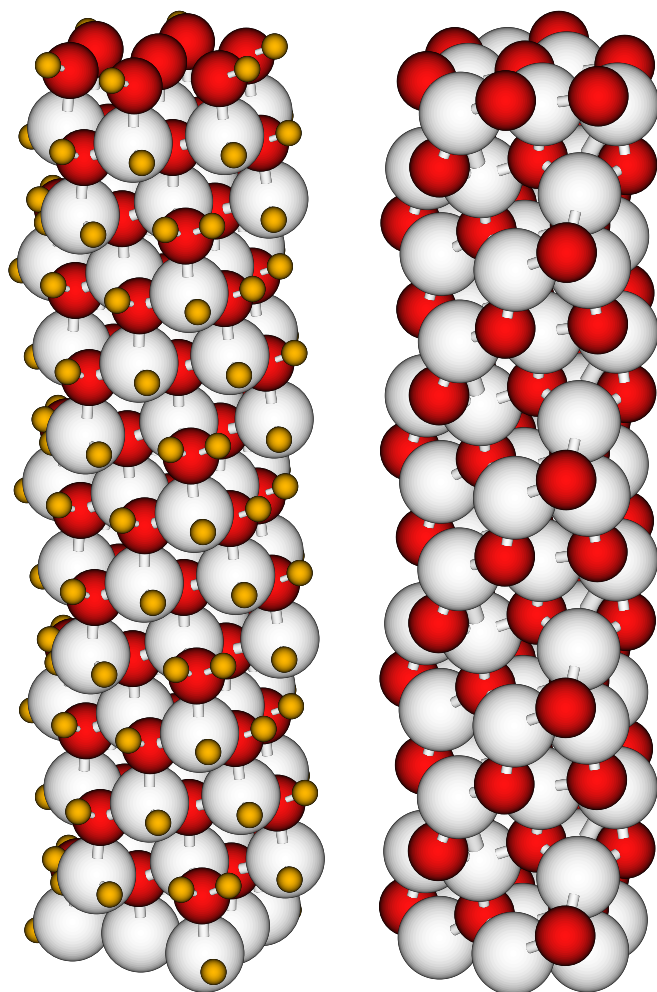


FIG. 1. (Color online) Atomic geometry of a H-passivated crystalline InP nanowire (left), and an unpassivated InP nanowire (right). The smallest (orange), the medium (red), and the bigger (white) balls represent the H, P, and In atoms, respectively.

face of the wire have been saturated by hydrogen atoms in such a way that all In and P atoms are fourfold coordinated (Fig. 1, left). In the other nanowire, starting from the H-passivated one, we just remove all H atoms from the nanowire surface. By permitting a full relaxation of the system, following the procedure described in the previous section, the surface In atoms of the optimized unpassivated nanowire are threefold or fourfold coordinated, and the In atoms inside the nanowire are fourfold, fivefold or even sixfold coordinated. Some of the In are linked with other In atoms (Fig. 1, right). The P atoms inside the nanowire are all fourfold coordinated and those on the surface are twofold or threefold coordinated. As reported before,²¹ nonsaturated nanowires introduce energy levels inside the band gap due to the surface dangling bonds. These surface levels affect the photoluminescence emission efficiency as observed recently.²² By comparing the nonrelaxed unpassivated nanowire (by just removing the H atoms from the H-passivated nanowire) with the fully relaxed unpassivated nanowire, we observe that the later one presents fewer energy bands inside the band gap. The diameter of the nanowires studied here are very thin,

around 1.3 nm, where the confinement and the effects due to the unpassivated surface will strongly affect their properties as compared to the bulk InP. For the H passivated nanowire, due to the confinement effects, the calculated band gap is enhanced in comparison to that of bulk InP.²³

The energetic stability of the Mn impurities can be examined by the calculation of well established concept of formation energy of defects (Ω_{Mn}). The formation energy of a Mn atom replacing an In atom in an InP system (bulk or nanocrystal) is given by

$$\Omega_{\text{Mn}} = E[\text{InP}_{\text{Mn}}] - E[\text{InP}] + n\mu_{\text{In}} - n\mu_{\text{Mn}},$$

where $E[\text{InP}_{\text{Mn}}]$ is the total energy of the InP system with the impurity and $E[\text{InP}]$ is the total energy of the defect free InP system. n denotes the number of In atoms replaced by Mn atoms. μ_{In} and μ_{Mn} are the In and Mn chemical potentials, respectively. The dependence of the formation energy with the Fermi energy is not taken into account since here we have always neutral defects. As we want only comparisons between formation energy of nanocrystals with respect to the bulk formation energy, we will not include the chemical potentials in the equation above, resulting in a relative formation energy.

Adjacent pairs of In atoms have been substituted by Mn atoms at several positions inside and on the surface of the InP nanowires. For most of the Mn pair configurations, the coordination number of the Mn remains the same of that of the removed In atoms, i.e., when the Mn are inside the nanowire they are fourfold, fivefold, or sixfold coordinated, and when the Mn are on the surface of the nanowire they are threefold or fourfold coordinated as will be shown later. The Mn pairs have always positioned at first neighbors In sites, keeping the Mn-Mn distances in a range between 3.7 and 4.4 Å (the distance depends on the impurity neighbor relaxations), in order that the magnetic coupling is more pronounced, since the Mn-Mn interaction is a short-range one in InP. As we reported before⁶ for H-passivated InP nanowires, the pairs of Mn atoms present lower formation energies when they are near to the surface of the nanowire. In Fig. 2, we plot the relative formation energy for a pair of Mn impurities as a function of the average Mn pair position with respect to the center of the nanowire. We observe that the formation energy for the H-passivated nanowire is higher than that of bulk InP. Also, we observe that the energy gain for the Mn atoms on the surface reach up to 0.3 eV per pair of Mn atoms, as compared to the Mn atoms in the center of the H-passivated nanowire. This is in agreement with recent theoretical results,¹⁶ where it has been shown that the Mn in nanocrystals have a self-purification mechanism, as the impurity prefers to migrate toward the surface.

On the other hand, for the unpassivated InP nanowire, our results show that the formation energy is lower than that of the bulk InP. When the Mn atoms are inside the nanowire (configurations U1–U5), the energy gain with respect to that of bulk InP is at the order of 1 eV or more, as we can see from Fig. 2. Also, we can observe from this figure that, contrary to what has been obtained for H-passivated nanowire, the Mn atoms do not migrate toward the surface. The most stable positions for the Mn are inside the nanowire and not

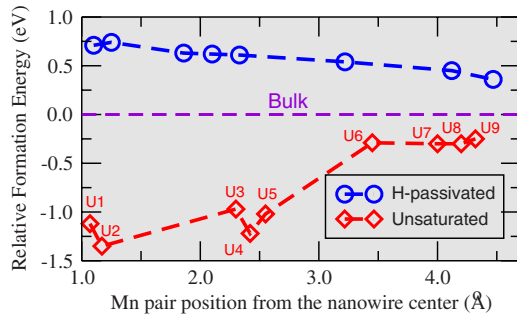


FIG. 2. (Color online) Relative formation energy of a pair of Mn atoms as a function of the Mn pair position with respect to the center of a H-passivated crystalline InP nanowire (circles), and an unpassivated nanowire (diamonds). The bulk defect formation energy is at the reference zero energy.

on the surface. However, even with the Mn atoms around the surface of the nanowire (configurations U6–U9) the formation energy is lower than the corresponding bulk defect for-

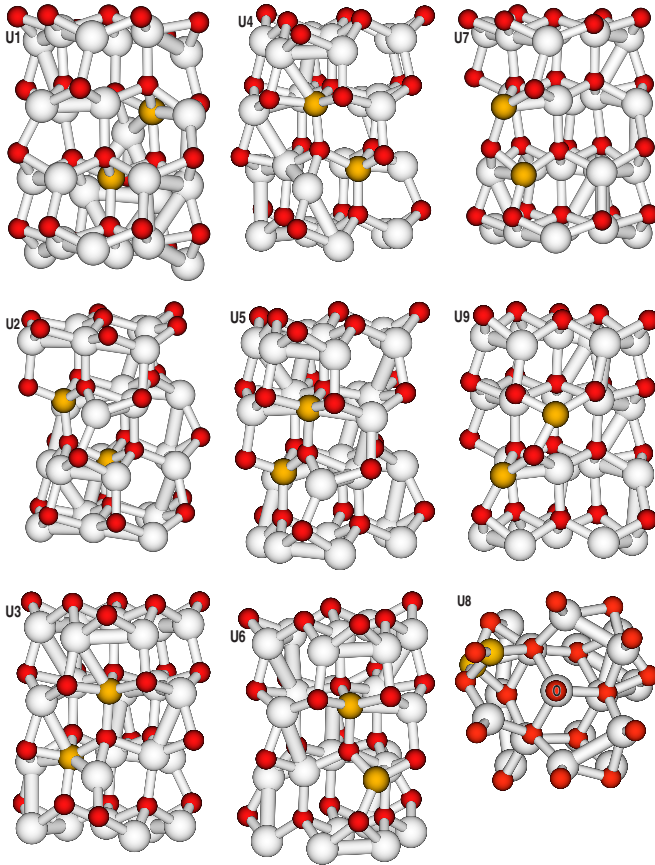


FIG. 3. (Color online) Schematic representation of the atomic positions when a pair of Mn atoms is substituted by In atoms in an unpassivated InP nanowire. The smaller (red), the medium (yellow), and the bigger (whiter) balls represent the P, Mn, and In atoms, respectively. The U8 configuration is a top view of the nanowire, {111} plane, where an axis along the [111] direction passing through the point marked with the O letter is used as the center of the nanowire to obtain the average position of the Mn atoms shown in Table I.

TABLE I. Mn-Mn exchange interaction energy ΔE (AFM-FM) (meV), magnetization in Bohr magnets, relative formation energy [ΔE_F (eV)] with respect to the bulk formation energy, and the average Mn pair position (in Å) with respect to the most central positioned Mn pair.

	ΔE (meV) (AFM-FM)	Mag (μ_B)	ΔE_F (eV)	d (Å)
U1	+18	2	0.00	1.07
U2	+502	2	-0.23	1.17
U3	-134	0	0.15	2.30
U4	+392	2	-0.10	2.42
U5	+287	2	0.10	2.55
U6	-65	0	0.81	3.45
U7	+131	10	0.82	4.00
U8	+126	10	0.82	4.20
U9	+6	10	0.87	4.32

mation energy. This result for the unpassivated nanowire is completely different from previous results of II-VI and IV-IV nanocrystals, where it has been shown that the Mn impurity prefers to migrate toward the surface of the nanocrystals.^{16,17} Here, for the unpassivated InP nanowire, besides the formation energy to be lower in the nanowire, there is a kind of barrier cap for the Mn atoms when they get closer to the surface, which can be attributed to a kind of amorphization of the nanowire surface, breaking the symmetry of the wire. In Fig. 3, the atomic arrangement for each Mn pair configuration is shown. It is interesting to know that some of the Mn atoms make bonds with In atoms. These Mn-In bond lengths are around 3 Å. The configurations that present ferromagnetic (FM) coupling and are not on the surface of the nanowire have at least one Mn atom not bounded to In atoms (U1, U2, U4, and U5). Those configurations where both Mn atoms are bounded to In atoms (U3 and U6) present antiferromagnetic (AFM) coupling. The configurations where both Mn atoms are around the surface of the wire present three bonds with P atoms plus one bond with In atom (U7, U8, and U9).

When the Mn atoms are located around the center of the H-passivated nanowire, as we reported before,⁶ the ferromagnetism is similar to the corresponding bulk InP, i.e., a FM parallel spins coupling is present. When the Mn atoms are located near the surface, there is either an AFM antiparallel spins coupling or no magnetic ordering. For the unpassivated InP nanowire, a different picture is obtained. The ground state presents mostly a FM coupling (see Table I) for the Mn atoms located inside or even on the surface of the nanowire. Also, it is important to stress that many FM configurations for the Mn pairs present an energy difference (AFM-FM) bigger than that of the bulk InP (+281 meV). The configurations that present the biggest FM coupling, labeled U2 and U4 in Fig. 2 and in Table I, are the most stable ones. Our results also show that the configurations that have high FM coupling present a magnetic moment of $2\mu_B$ instead of $8\mu_B$ as obtained for bulk InP and for the H-passivated nanowire. This reduction of the magnetic moment is due to the presence of minority spin states inside the nanowire band

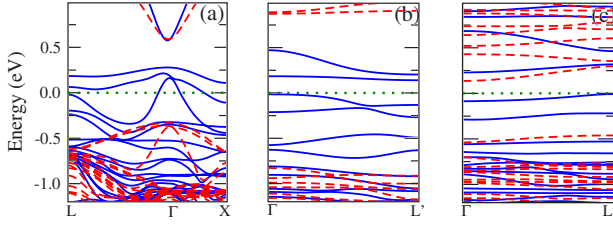


FIG. 4. (Color online) Spin-polarized energy bands for a pair of Mn doped (a) bulk InP, (b) H-passivated InP nanowire with FM coupling, and (c) unpassivated InP nanowire (configuration U7 from Table I). Full (blue) lines represent the majority spin, while dashed (red) lines represent the minority spin. The horizontal dotted (green) line is the Fermi energy.

gap, as shown in Fig. 4. For an isolated Mn doped bulk InP, the majority spin states at the valence band maximum (VBM) are partially occupied. When two Mn atoms have been added in our supercell leading to a Mn concentration of 3%, as we can see from Fig. 4(a), the heavy holes states, initially double degenerated, split up. The Fermi energy is not localized in a Mn-induced impurity band as suggested to be in Mn doped GaAs,¹⁵ but the Fermi energy is positioned inside the valence band, crossing the light and heavy hole bands (this may be a result from the fact that the Mn is substituted at In sites). This result is similar to a calculation of Mn in GaAs, where the Fermi energy lies in a partially occupied three-degenerate state.¹³ As we can see in Fig. 5, for Mn doped bulk InP, the d electrons of the Mn atoms are located around 3.0 eV deep inside the valence band, leaving holes at the VBM, resulting in a net magnetic moment of $4\mu_B$ per Mn atom. The holes at the VBM present a stronger host p character with some contributions of the Mn d component for both FM and AFM couplings. The energetically most stable FM coupling for bulk InP is a half metallic system, as can be seen in Figs. 4(a) and 5(a).

For the H-passivated nanowire, the origin of the ferromagnetism is similar to the one applied to the corresponding bulk InP; however, due to confinement effects, the hole states are more localized as can be observed by comparing Fig. 4(a) with Fig. 4(b). The band structure shown in Fig. 4(b) is a FM coupling configuration with both Mn atoms placed at most center position of the nanowire. This picture for the H passivated nanowire favors a double exchange mechanism, which involves localized holes, similarly as has been proposed for GaAs.¹⁵ However from Fig. 4(b), we observe that the highest occupied molecular orbital (HOMO) presents some energy dispersion. The last occupied energy bands as well the first unoccupied energy bands are all one channel spin; however, we cannot state that this system is half metallic since the levels in the gap are very localized.

On the other hand, the ferromagnetism of the unpassivated nanowire has some peculiar differences. The surface introduces a lot of states inside the band gap. In Fig. 4(c), the band structure for the configuration U7 is plotted. The states inside the band gap interact with the acceptor levels, leading to two types of FM coupling with a net magnetic moment of $10\mu_B$ and $2\mu_B$. As we mention before, the lower magnetic moment is due to the presence of minority spin states inside the band gap. In Fig. 6, we can see that when a FM coupling

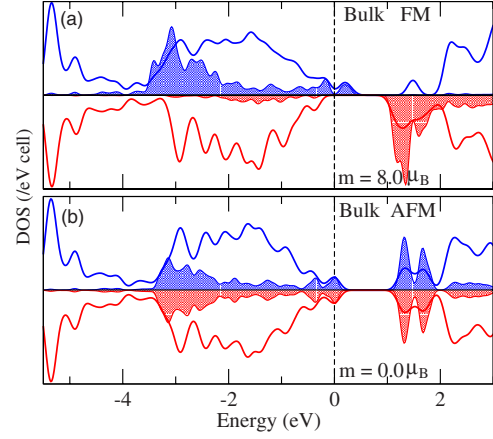


FIG. 5. (Color online) Total density of states (full lines) and partial density of states projected into Mn d orbitals (filled to base lines) for bulk InP with (a) FM coupling and (b) AFM coupling. For each plot, the spin is split into up (blue above) and down (red below). The vertical dashed line is the Fermi energy. The projected d density is five times the total DOS.

is present the HOMO is a majority spin, while for the AFM coupling, the HOMO is a minority spin. The Mn d electrons are also deep inside the valence band, mainly for the magnetization $m=10\mu_B$. For $m=2\mu_B$, the d contributions are not very localized, but they are distributed inside the VB and conduction band. For the AFM coupling, the Mn d electrons distribution is not symmetric as is observed in bulk InP. This result is due to the break of the crystal symmetry, where Mn make bonds with In atoms. As the Mn states are localized, usually they are less affected by confinement effects, as has been observed in GaAs (Ref. 24) and in our InP passivated nanowire.⁶ However, here, for this unpassivated nanowire, the surface states inside the band gap interact with the delocalized host states leading to a FM coupling by surface states.

In order to verify the localization of the magnetic moment in this unpassivated InP nanowire, we plot in Fig. 7 the net magnetization $m(\mathbf{r})=\rho_{\uparrow}(\mathbf{r})-\rho_{\downarrow}(\mathbf{r})$, where $\rho_{\uparrow(\downarrow)}$ is the total charge density in the $\uparrow(\downarrow)$ -polarized channel. The $m(\mathbf{r})$ plot is for a FM coupling, with a magnetic moment of $10\mu_B$ (configuration U7 from Table I), containing two Mn atoms, represented by the biggest (green) balls in Fig. 6. The spin densities are more localized around the Mn sites, but also we can see some magnetization with d_{\uparrow} -like character [darker (blue) charge in Fig. 7] on the surface of the nanowire. Close to the P neighbors, the character changes to p_{\downarrow} -like. The FM coupling is guided by the surface states, which cannot be ascribed to a Zener-like picture through delocalized holes as is observed in bulk InP [see Fig. 4(a)], neither within a RKKY since there are no free carriers. In this unpassivated InP nanowire, we can see some localized deep states below the VBM [see Fig. 4(c)], and the FM coupling is via surface states.

IV. CONCLUSION

In summary, our calculations show that Mn doped unpassivated InP nanowires present desired properties for spin-

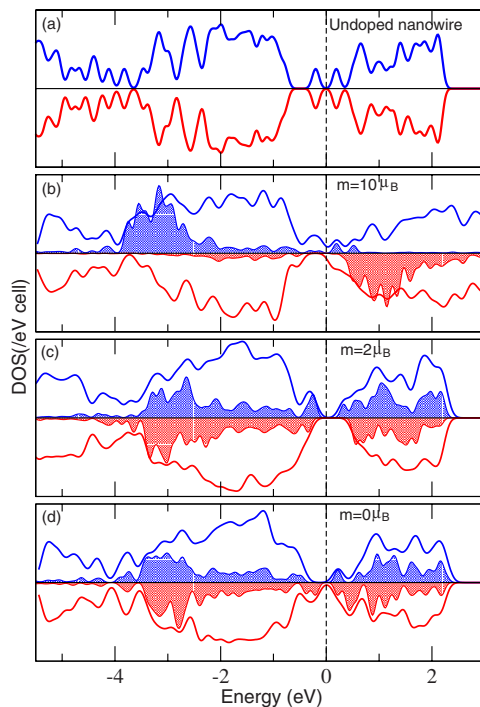


FIG. 6. (Color online) Total density of states (full lines) and partial density of states projected into Mn d orbitals (filled to baselines) for (a) an unpassivated InP nanowire, two Mn atoms (b) with FM coupling (configuration U7 from Table I), (c) with FM coupling (configuration U2 from Table I), and (d) with AFM coupling (configuration U3 from Table I). For each plot, the spin is split into up (blue above) and down (red below). The vertical dashed line is the Fermi energy. The projected d density is five times the total DOS.

tronic applications. The Mn substituted at In sites present lower formation energies in unpassivated nanowires than in bulk InP, and the Mn atoms prefer to be inside the nanowire and not on the surface. The self-purification mechanism is

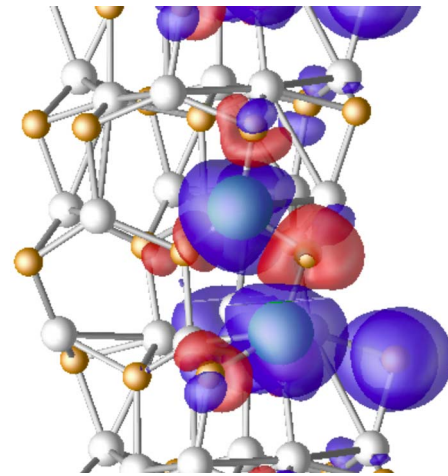


FIG. 7. (Color online) Net magnetization $m(\mathbf{r}) = \rho_{\uparrow}(\mathbf{r}) - \rho_{\downarrow}(\mathbf{r})$ for the FM coupling, configuration U7. Darker (blue) regions represent the ρ_{\uparrow} , while the lighter (red) regions represent the ρ_{\downarrow} electronic densities. The smallest (orange), the intermediate (white), and the bigger (green) balls represent the P, In, and Mn atoms, respectively.

not present in this unpassivated III-V nanowire. We found that most of the Mn pair configurations present FM coupling, with the Mn atoms inside or on the surface of the unpassivated nanowire. Different from the bulk, the Mn atoms introduce localized impurity bands inside the band gap, leading to a stabilization of the FM interaction via surface states. Our results also show that the stability of the ferromagnetism is stronger in the nanowire as compared to that of bulk InP.

ACKNOWLEDGMENTS

This work was supported by the Brazilian agencies FAPEMIG and CNPq.

- ¹H. Ohno, H. Munekata, T. Penney, S. von Molnar, and L. L. Chang, *Phys. Rev. Lett.* **68**, 2664 (1992).
- ²H. Ohno, *Science* **281**, 951 (1998).
- ³A. H. Macdonald, P. Schiffer, and N. Samarth, *Nat. Mater.* **4**, 195 (2005).
- ⁴P. Poddar, Y. Sahoo, H. Srikanth, and P. N. Prasad, *Appl. Phys. Lett.* **87**, 062506 (2005).
- ⁵K. Somaskandan, G. M. Tsoi, L. E. Wenger, and S. L. Brock, *Chem. Mater.* **17**, 1190 (2005).
- ⁶T. M. Schmidt, P. Venezuela, J. T. Arantes, and A. Fazzio, *Phys. Rev. B* **73**, 235330 (2006).
- ⁷P. V. Radovanovic, C. J. Barrelet, S. Gradeak, F. Qian, and C. M. Lieber, *Nano Lett.* **5**, 1407 (2005).
- ⁸D. S. Han, J. Park, K. W. Rhie, S. Kim, and J. Chang, *Appl. Phys. Lett.* **86**, 032506 (2005).
- ⁹Y. Cui, Q. Wei, H. Parker, and C. M. Lieber, *Science* **293**, 1289 (2001).
- ¹⁰X. Duan, Y. Huang, Y. Cui, J. Wang, and C. M. Lieber, *Nature*

- (London) **409**, 66 (2001).
- ¹¹K. Sato, W. Schweika, P. H. Dederichs, and H. Katayama-Yoshida, *Phys. Rev. B* **70**, 201202(R) (2004).
- ¹²G. M. Dalpian and Su-Huai Wei, *J. Appl. Phys.* **98**, 083905 (2005).
- ¹³P. Mahadevan, A. Zunger, and D. D. Sarma, *Phys. Rev. Lett.* **93**, 177201 (2004).
- ¹⁴A. J. R. daSilva, A. Fazzio, R. R. dos Santos, and L. E. Oliveira, *Phys. Rev. B* **72**, 125208 (2005).
- ¹⁵K. S. Burch, D. B. Shrekenhamer, E. J. Singley, J. Stephens, B. L. Sheu, R. K. Kawakami, P. Schiffer, N. Samarth, D. D. Awschalom, and D. N. Basov, *Phys. Rev. Lett.* **97**, 087208 (2006).
- ¹⁶G. M. Dalpian and J. R. Chelikowsky, *Phys. Rev. Lett.* **96**, 226802 (2006).
- ¹⁷S. C. Erwin, L. Zu, M. I. Haftel, A. L. Efros, T. A. Kennedy, and D. J. Norris, *Nature* (London) **436**, 91 (2005).
- ¹⁸T. Dietl, H. Ohno, F. Matsukura, J. Cibert, and D. Ferrand, *Science* **287**, 1019 (2000).

- ¹⁹D. Vanderbilt, Phys. Rev. B **41**, R7892 (1990).
- ²⁰G. Kresse and J. Hafner, Phys. Rev. B **47**, R558 (1993); G. Kresse and J. Furthmüller, *ibid.* **54**, 11169 (1996).
- ²¹T. M. Schmidt, Appl. Phys. Lett. **89**, 123117 (2006).
- ²²M. Mattila, T. Hakkarainen, H. Lipsanen, H. Jiang, and E. I. Kauppinen, Appl. Phys. Lett. **90**, 033101 (2007).
- ²³T. M. Schmidt, R. H. Miwa, P. Venezuela, and A. Fazio, Phys. Rev. B **72**, 193404 (2005).
- ²⁴X. Huang, A. Makmal, J. Chelikowsky, and L. Kronik, Phys. Rev. Lett. **94**, 236801 (2005).